

2002

Morphology and Effects of Hydrogen Etchings of Porous SiC

Ashutosh Sagar
Carnegie Mellon University

C. D. Lee
Carnegie Mellon University

Randall M. Feenstra
Carnegie Mellon University, feenstra@andrew.cmu.edu

C. K. Inoki
SUNY Albany

T. S. Kuan
SUNY Albany

Follow this and additional works at: <http://repository.cmu.edu/physics>

Published In

J. Appl. Phys., 92, 4070.

This Article is brought to you for free and open access by the Mellon College of Science at Research Showcase @ CMU. It has been accepted for inclusion in Department of Physics by an authorized administrator of Research Showcase @ CMU. For more information, please contact research-showcase@andrew.cmu.edu.

Morphology and Effects of Hydrogen Etching of Porous SiC

Ashutosh Sagar, C. D. Lee and R. M. Feenstra

Department of Physics, Carnegie Mellon University, Pittsburgh, PA 15213

C. K. Inoki and T. S. Kuan

Department of Physics, University at Albany, SUNY, Albany, NY 12222

Abstract

The morphology of the porous network in porous SiC has been studied. It has been found that pore formation starts with a few pores on the surface and then the porous network grows in a V-shaped branched structure below the surface. The hydrogen etching rates of porous and nonporous SiC have been measured. Etch rates of porous and nonporous wafers of various miscuts are found to be equal within a factor of two, indicating that the rate-limiting step in the etching process arises from the supply of active etching species from the gas phase. The porous SiC etches slightly faster than the nonporous SiC, which is interpreted simply in terms of the reduced average density of the porous material.

I. Introduction

The technique of photo-electrochemical (PEC) etching of n-type SiC has been studied extensively. J. S. Shor conducted a series of experiments in the early 1990's to study the PEC etching of SiC [1]. Soon thereafter, the formation of porous SiC by PEC etching was reported [2]. Anodizing n-type 6H SiC in hydrofluoric acid (HF) under ultra-violet illumination formed porous SiC. Pores in the range of 10 to 30 nm diameter with the inter-pore spacing from 5 to 150 nm were observed by transmission electron microscopy (TEM). Currently, porous SiC is becoming an attractive candidate as a substrate for epitaxy with the porous network providing potential defect reduction and strain relaxation in epitaxial films [3-5]. Porous GaN has also been investigated for similar reasons [6].

In this work we have observed the surface pores and the underlying porous network in porous SiC using scanning electron microscopy (SEM) and TEM. In addition, we have studied the effects of high temperature hydrogen etching on the porous SiC. Hydrogen etching is often used to remove surface damage from as-received SiC wafers and prepare large atomically flat surfaces [7-10]. The method involves exposing the SiC surface to hydrogen at temperatures of 1600-1700°C. Here, we report results for the hydrogen etch rate as a function of temperature for both nonporous and porous SiC of various miscuts, and we also discuss the morphology of the etched porous layers.

II. Experiment

The porous SiC samples studied in this work were purchased from TDI, Inc. They were prepared by anodization at current density of 7 mA/cm² for 3 min, with a 250 watt

Hg lamp illuminating the 2 inch diameter wafers. We have acquired plan-view and cross-sectional SEM images of the porous layers. For the latter, samples were fractured to expose a cross-sectional surface. The samples were cleaned with acetone and then dried with nitrogen. They were examined with a Philips field emission gun SEM at an accelerating voltage of 15 kV. TEM observations were performed on a JEOL JEM200CX electron microscope operating at 200 kV. We used three different types of Si-face (0001)-oriented SiC wafers: 6H with no intentional miscut (i.e. on-axis), 6H with 3.5° miscut, and 4H with 8° miscut. In the latter two cases the miscut is towards the $[11\bar{2}0]$ direction. The wafers were n-type with resistivities in the range 0.03–0.17 ohm-cm for 6H and 0.04–0.05 ohm-cm for 4H material. We have examined the porous morphology of nine different wafers; the morphologies were found to vary with the resistivity of the material, as described in section III. A.

Hydrogen etching was performed at three different temperatures, 1600°C, 1680°C and 1720°C, as measured on the nonporous side of each sample. The surface temperature of the sample was monitored by a disappearing filament optical pyrometer. The sample was mounted on a tantalum strip. A current of 40 - 45 A was passed through the strip to heat up the strip and sample. During etching the hydrogen flow (99.99% pure) is maintained at 11.3 l/min through an etching chamber at 1 atm pressure.

For the H-etching experiments we used wafers which had been anodized on only one half of their area. During H-etching the porous side of the sample was found to etch faster than the nonporous side, thereby creating a step at the porous-nonporous boundary. The height of this step was measured with an optical profiler to determine the etch rates. This instrument works like a Michelson interferometer: the sample is placed as one of the mirrors and white light fringe patterns were produced by finely adjusting the tilt of the sample. This pattern is seen real time through a video camera. Then the objective moves vertically through a certain distance (20 μm) to map the fringe pattern over the entire field of view. A 2D constant-height contour plot of the surface is obtained.

III. Results and Discussion

A. Morphology

Figure 1 shows an SEM image of a fractured porous 6H-SiC layer, revealing surface pores and the underlying porous network. It is clear from this image that the porosity of the bulk porous network is much greater than that on the surface. TEM bright-field images of similar porous layers on other 6H wafers are shown in Figs. 2(a) and (b). From such TEM and SEM images we find a pore size (i.e. minimum distance across a pore) of about 20 nm and a bulk porosity of typically 20–30% for the layers studied here. From Fig. 2 it is seen that the pores grow downwards in a highly branched structure. In these cross-sectional images the pores have the appearance of partially open cones. The angle between the upper cone sidewall and a line normal to the (0001) surface is about 75° near the surface, decreasing to 55° at a depth of about 1.5 μm into a porous layer. Similar results are obtained for 4H material, with facets angles of about 65° near the surface and 45° at a depth of 1.5 μm . Near the top surface, where the pore formation has just begun, the porous network is not very dense, leading to the existence of a thin nonporous skin layer. This ≈ 50 nm thick skin layer is clearly seen in the TEM image of

Fig. 2(a). The pores start to form a dense network only below this skin layer. The general morphology of the porous network described above is quite similar to that observed by Zangoie *et al.* [11].

In Fig. 3(a) we show a plan-view SEM image of the porous network. Pores of about 25 nm diameter are visible. The top surface pore density in this case is $50 \pm 2 \mu\text{m}^{-2}$. For all the porous layers studied here we find similar size surface pores, with the surface porosity varying between 1 and 3% from sample to sample. Reactive ion etching (RIE) was used to see the growth of the subsurface porous structure in plan view. A porous SiC sample was etched in a rf-generated (250 W) SF_6 plasma for 2 minutes. Gas flow was maintained at 30 sccm at 20 mTorr pressure. This process removed about 100 nm of material thus eliminating the skin layer. A plan-view SEM image of this surface is shown in Fig. 3(b) where one can see a very dense porous network. It is useful to compare this image with one shown below [Fig. 4(c)] for a higher resistivity sample in which the pores and connecting channels are more clearly visible.

The results presented above are typical of majority of our wafers studied, which have resistivities of $0.03 - 0.05 \Omega\text{-cm}$. In contrast, samples with higher resistivities of $0.13 - 0.17 \Omega\text{-cm}$ have a somewhat different porous morphology as shown in Fig. 4. We see there large diameter pores surrounded by a relatively sparse porous network. Similar results about porous Si have been reported before [12,13]. The cross-sectional TEM image of Fig. 4(a) clearly shows this morphology, and the cross-sectional SEM image of Fig. 4(b) similarly shows the large pores. Figure 4(c) shows a plan-view SEM image of the same sample after it was subjected to a SF_6 rf-plasma etch for 6 minutes thereby removing the skin layer. Figure 4(c) reveals a branched network extending laterally away from central cores. The branched structure seen in Fig. 4(c) provides useful insight into the formation mechanism for the porous layers [12,13]. We believe that a similar branching morphology occurs in our other (i.e. lower resistivity) samples, but the network in those cases is more dense.

As mentioned in the introduction, H-etching is used to remove polishing damage from SiC wafers, thereby producing atomically flat surfaces [9,10]. The H-etching also changes the morphology of the porous network as discussed below. Figure 5 shows a plan-view SEM image of a 4H-SiC sample after H-etching for 60 seconds at 1680°C . The pores have clearly opened up after the etching process (identical results were obtained on 6H-SiC). We have measured the effect of H-etching on the surface porosity. The average size of the pores in Fig. 5 is about 100 nm, corresponding to a surface porosity of about 3.5%. Additional H-etching causes the surface porosity to increase further and it also modifies the bulk pore structure. Figure 6(a) is a cross-sectional image of the same sample etched for 60 seconds. It is clear that the bulk pores have opened up after the etching process and the network morphology is changed from an unetched sample. The bulk porosity after 60 seconds of H-etch time was about 18% and the average pore size is about 100 nm. After 120 seconds of H-etch time the bulk porosity increased to about 24% and after 300 seconds of etching the bulk porosity was 31%. The latter case is shown in Fig. 6(b). These observations indicate that the etching process opens up the pores more and more with longer etching time. The resulting increase in porosity has an effect on the

H-etching rate of porous SiC as discussed in the following section. Greater porosity provides lesser surface area for etching per plane and therefore the etch rate increases.

B. Etch Rates

To measure the hydrogen-etch rates we used samples that were made porous on half of the wafer and nonporous on the other half. After H-etching, due to a difference in etch rates there is a height difference between the two sides as measured by optical profilometry. The height difference is plotted as a function of etching time in Fig. 7 for three different samples and three different temperatures. The temperatures were measured on the nonporous part of each sample. We found that for a given current density through the tantalum foil (during H-etching) and hydrogen flow rate, the porous side shows a higher temperature by about 40°C, as estimated by the optical pyrometer [14].

Each of the plots in Fig. 7 shows a final plateau. At this stage the entire porous layer has been removed. We know the porous layer thickness for each of these cases from SEM. From the ratio of layer thickness to time to reach the plateau, we calculate the average etching rate of the porous material. Then, from the final height difference between porous and nonporous layers we know the thickness of nonporous material removed and we thus obtain its average etching rate. These results are given in Table I for samples of three different miscuts.

The etching rates of nonporous SiC show a definite increase between 1600°C and higher temperatures, but the difference in etching rates between 1680°C and 1720°C is not significant. Thus we conclude that the etching rate saturates at the higher temperature. No observable difference in etching rates of porous SiC was observed between all three temperatures studied. However, as mentioned above, the porous side was at a higher temperature than the nonporous side for given etching conditions. We thus consider it likely that the porous side is etching in the saturation range at all three temperatures studied.

It is notable that all our observed etching rates, at higher temperature (i.e. not including the 1600°C results from the nonporous material), are within a factor of two of each other. This near equality persists despite the fact that the surface morphology arising from the surface miscut is much different in each case. Different miscuts lead to vastly different step densities and kink densities on various surfaces [10]. Thus, we conclude that these step or kink densities do *not* determine the etching rate. On the other hand, etching *does* seem to occur at step edges, since images of etched surface do not reveal pits and other features which could result from homogeneous etching of the (0001) surface [9]. Since the step density does not determine the etching rate, we therefore surmise that the supply of active etching species from the gas phase (or the rate of reaction of these species) must somehow be determining the observed etch rates. We note that the temperature at which the H-etching rates saturate is close to that used by filaments which dissociate H₂ [15]. Thus it seems likely that the etching rates are limited by the concentration of H atoms, as determined by the equilibrium between the H₂ dissociation and recombination rates at the surface.

To date we have performed etching only with pure H₂ gas, so we do not have any data regarding the efficacy of different gas species in the etching process. We know that one other group has used diluted H₂ (mixed with He) for their etching [16]; etching rates were not reported, although qualitatively the results appear to be similar to those described here. Further experiments are needed to clarify the chemistry of the etching process. From the point of view of the processing tool, however, the present results of nearly constant etch rates independent of surface miscut and porosity are quite simple and useful.

Further examining the results in Table 1, we note that for the nonporous material at temperatures of 1680°C and above, the etch rates of the 4H material are consistently lower than those of the 6H material. On the average, the ratio of 4H to 6H etch rates is 0.72. This result is quite close to the ratio of unit cell heights (i.e. in the (0001) direction) of the two materials, namely $4/6 = 0.67$. Since etching occurs in integral layers of unit cell height, our result follows what would be expected provided that all other factors affecting the etch rate are constant between the two polytypes.

We find that the etching rate of porous SiC is nonlinear in time, as seen for example in the plot for the 0° miscut sample at 1600°C in Fig. 7. The etching rate is found to increase with time. One source of this effect may be the gradual increase in pore size with etching time. Since less material exists on a given horizontal cross-sectional plane, the etching time per plane will decrease (assuming that the etching time is proportional to the area of the cross-sectional plane occupied by SiC, as indicated by the above discussion). As mentioned in the previous section the bulk porosity increases with time, being 18%, 24%, and 31% after 60 s, 120 s, and 300 s, respectively, of etch time. Figures 6(a) and (b) show cross-sectional SEM images of porous SiC etched at 1680°C for 60 seconds and 300 seconds, respectively. The increasing pore size is clearly evident there. From Table 1 we find that, on average, the etch rates for the porous material is about 50% higher than the nonporous material. At the start of the etching the bulk porosity of the layer is 15-20%, and during the etch we find that pores open up and the porosity increases to 30% or more after 300 seconds of etching. Denoting the bulk porosity as P , then the occupied area per atomic plane will be proportional to $1-P$ and the etch rate to $1/(1-P)$. The observed nonlinearity in the etching rates qualitatively follow that expected from this dependence, and indeed, the overall increase in the etch rate of the porous layers compared to the nonporous layers is also consistent with this dependence.

Finally, we note that for the highest temperature (1720° C) etching results in Fig. 7, the etching appears to be rather linear. We do not have definitive data to interpret this change, but we suggest that morphology of the porous network during etching is somewhat different at the highest temperature than for lower temperature and this affects the etching process. As indicated in Fig. 6(b) (for etching temperature of 1680°C), the pores form open voids below the surface but near the surface there is a layer where the density of pores is reduced. It appears that, near the surface, vacancies from the voids diffuse directly out of the surface. Coarsening of the porous network may in fact produce closed voids, so that they do not grow in size with time. In this case, the presence of the

subsurface voids will affect the etch rate only insofar as they yield vacancies to the surface, and the resulting etch rates may indeed be linear with time.

IV. Conclusions

We have observed the pore size and porosity of porous SiC using SEM and TEM. The images reveal a thin skin layer above the porous network. The morphology of the porous network was found to vary with the resistivity of the material. H-etching of porous and nonporous material has been studied and etch rates have been measured. It was found that the etching rate depends upon porosity, and it was observed that etching process opens up the pores. Etch rates of porous and nonporous wafers of various surface miscuts are found to be equal within a factor of two, indicating that the rate-limiting step in the etching process arises from the supply of active etching species from the gas phase.

Acknowledgements

This work was supported by a Defense University Research Initiative on Nanotechnology (DURINT) program administered by the Office Naval Research under Grant N00014-01-1-0715 (program monitor C. Wood). Discussions with W. J. Choyke, R. P. Devaty, and M. Mynbaeva are gratefully acknowledged.

References

- [1] J. S. Shor and R. M. Osgood Jr., J. Electrochem. Soc. **140**, L123 (1993).
- [2] J. S. Shor, I. Grimberg, B.-Z. Weiss and A. D. Kurtz, Appl. Phys. Lett. **62**, 2836 (1993).
- [3] S. E. Sadow, M. Mynbaeva, W. J. Choyke, S. Bai, G. Melnychuk, Y. Koshka, V. Dimitriev and C. E. C. Wood, Mater. Science Forum **353 - 356**, 115 (2001).
- [4] M. Mynbaeva, A. Titkov, A. Kryzhanovski, V. Ratnikov, H. Huhtinen, R. Laiho and V. Dimitriev, Appl. Phys. Lett. **76**, 1113 (2000).
- [5] G. Melnychuk, M. Mynbaeva, S. Rendakova, V. Dimitriev and S. E. Sadow, Mat. Res. Soc. Symp. Vol. **622**, T4.2.1 (2000).
- [6] X. Li, Y.-W. Kim, P. W. Bohn, I. Adesida, Appl. Phys. Lett. **80**, 980 (2002).

- [7] C. Hallin, A. S. Bakin, F. Owman, P. Martensson, O. Kordina, E. Janzen, *Silicon Carbide and Related Materials* 1995, Kyoto, Japan, Inst. Phys. Conf. Ser. No. **142**, Chapter 3, 1996 IPO Publishing Ltd.
- [8] T. L. Chu and R. B. Cambell, J. Electrochem. Soc. **112**, 995 (1965).
- [9] V. Ramachandran, M. F. Brady, A. R. Smith and R. M. Feenstra, J. Electron. Mat. **27**, 308 (1998).
- [10] C. D. Lee, R. M. Feenstra, O. Shigiltchoff, R. P. Devaty and W. J. Choyke, MRS Internet J. Nitride Semicond. Res. **7**, 2 (2002).
- [11] S. Zangoie, J. A. Woollam and H. Arwin, J. Mater. Res. **15**, 1860 (2000).
- [12] R. L. Smith and S. D. Collins, J. Appl. Phys. **71**, R1 (1992).
- [13] A. Valance, Phys. Rev. B **52**, 8323 (1995)
- [14] This temperature difference between the porous and nonporous sides of the sample is also apparent from the results of GaN growth on the SiC, in which the GaN on the porous side had morphology indicative of lower surface coverage of Ga. An identical change in the surface morphology can be achieved by a $\approx 40^\circ\text{C}$ increase in sample temperature which increases the Ga desorption rate from the surface. [C. D. Lee, V. Ramachandran, A. Sagar, R. M. Feenstra, D. W. Greve, W. L. Sarney, L. Salamanca-Riba, D. C. Look, Song Bai, W. J. Choyke and R. P. Devaty, J. Electron. Mat. **30**, 162 (2001)].
- [15] U. Bischler and E. Bertel. J. Vac. Sci. Technol. A **11**, 458 (1993).
- [16] V. M. Torres, J. L. Edwards, B. J. Wilkens, D. J. Smith, R. B. Doak and I. S. T. Tsong, Appl. Phys. Lett. **74**, 985 (2001).

Table I. H-etching rates of porous and nonporous SiC. The etching rates have typical uncertainty of $\pm 10\%$.

Sample	Nonporous SiC etch rate (nm/sec)			Porous SiC etch rate (nm/sec)		
	1600°C	1680°C	1720°C	1600°C	1680°C	1720°C
6H, on-axis	0.6	1.1	1.2	1.7	1.2	1.8
6H, 3.5° miscut	0.4	1.1	1.0	1.9	1.7	1.5
4H, 8° miscut	0.84	0.85	0.73	1.6	1.5	1.2

^a Reported temperatures correspond to that of the nonporous material. As discussed in the text, the porous side of the wafers showed a higher temperature than the nonporous side by about 40°C.

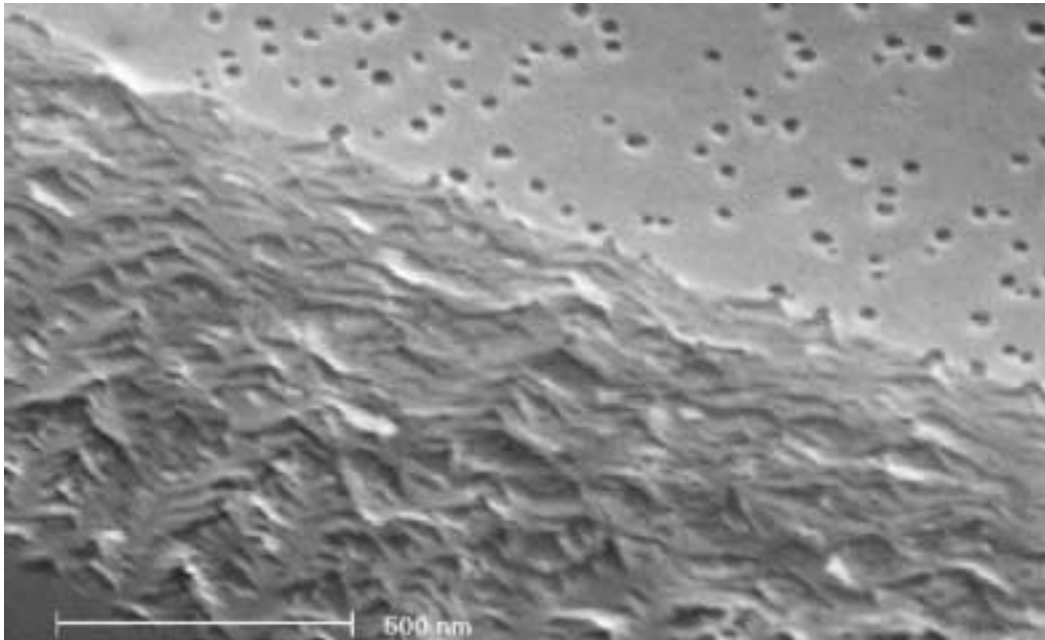


Figure 1. SEM image of porous 6H-SiC. The sample was tilted to allow simultaneous viewing of the porous network in cross-section and the pores on the top surface. Pore formation started at the surface and then it develops into a V-shaped branched structure below the surface. The scale marker shows a length of 500 nm.

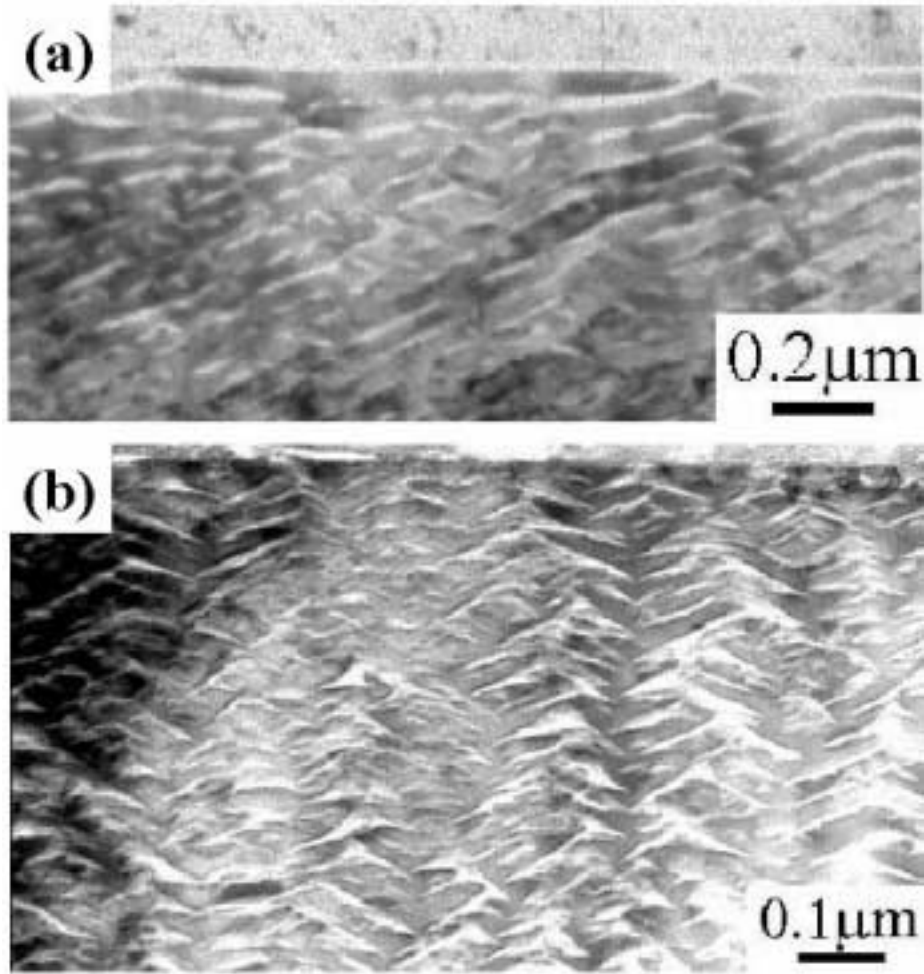


Figure 2. Cross-sectional TEM images of two porous 6H-SiC layers. There are very few pores on the surface. The top skin layer is most clearly visible in (a). The V-shaped branched structure of the porous network is most clearly seen in (b). The sample resistivity 0.032 Ω -cm.

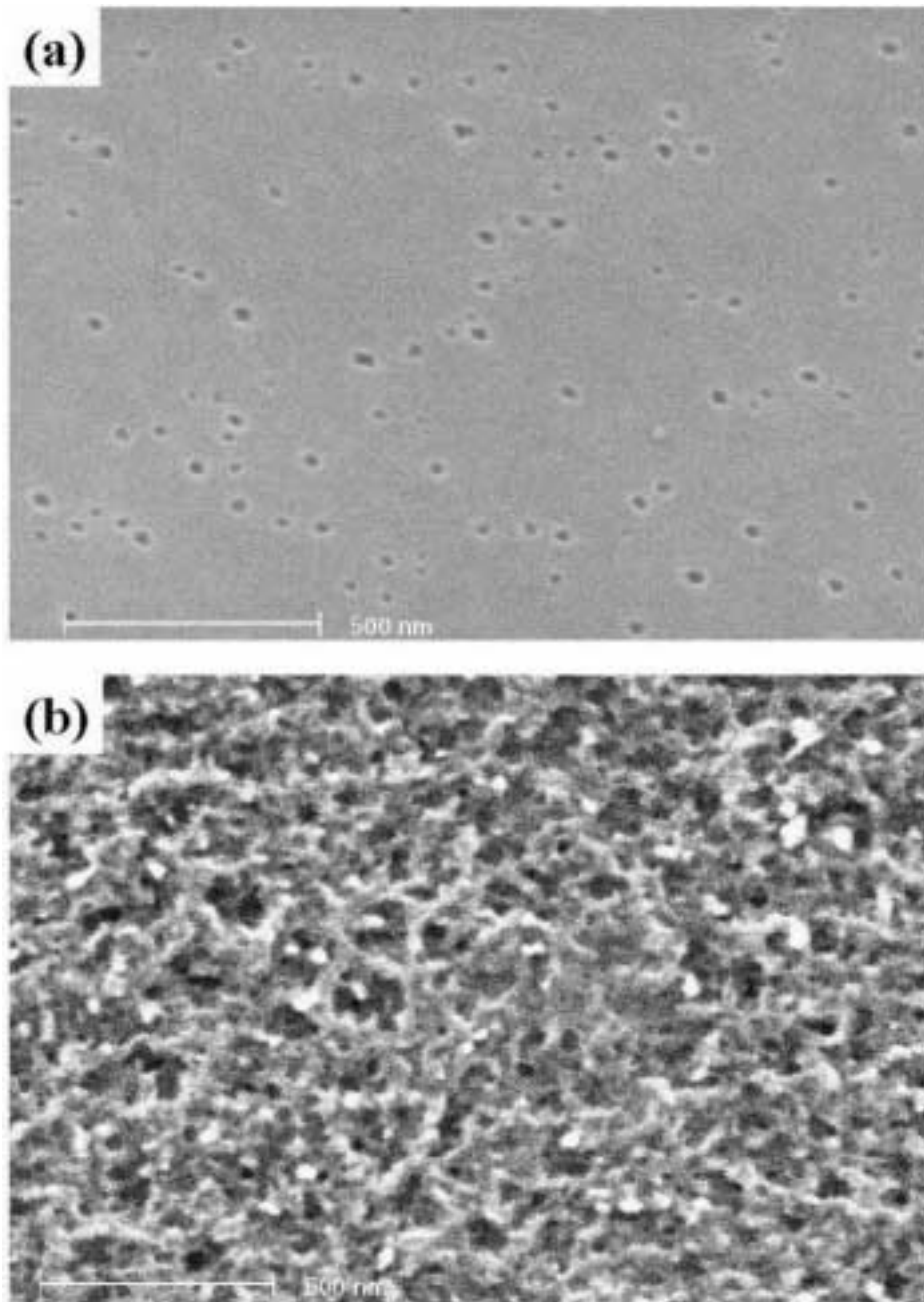


Figure 3. (a) Plan-view SEM image of porous 6H-SiC. Pores of about 30 nm diameters are seen here. The white cloudy features arise from residual surface contamination. The scale marker shows a length of 500 nm. (b) A plan view image of the porous 6H-SiC sample surface as in (a), which has been reactive ion etched to remove about 100 nm from the surface. The scale marker shows a length of 500 nm. The sample resistivity is $0.032 \Omega\text{-cm}$.

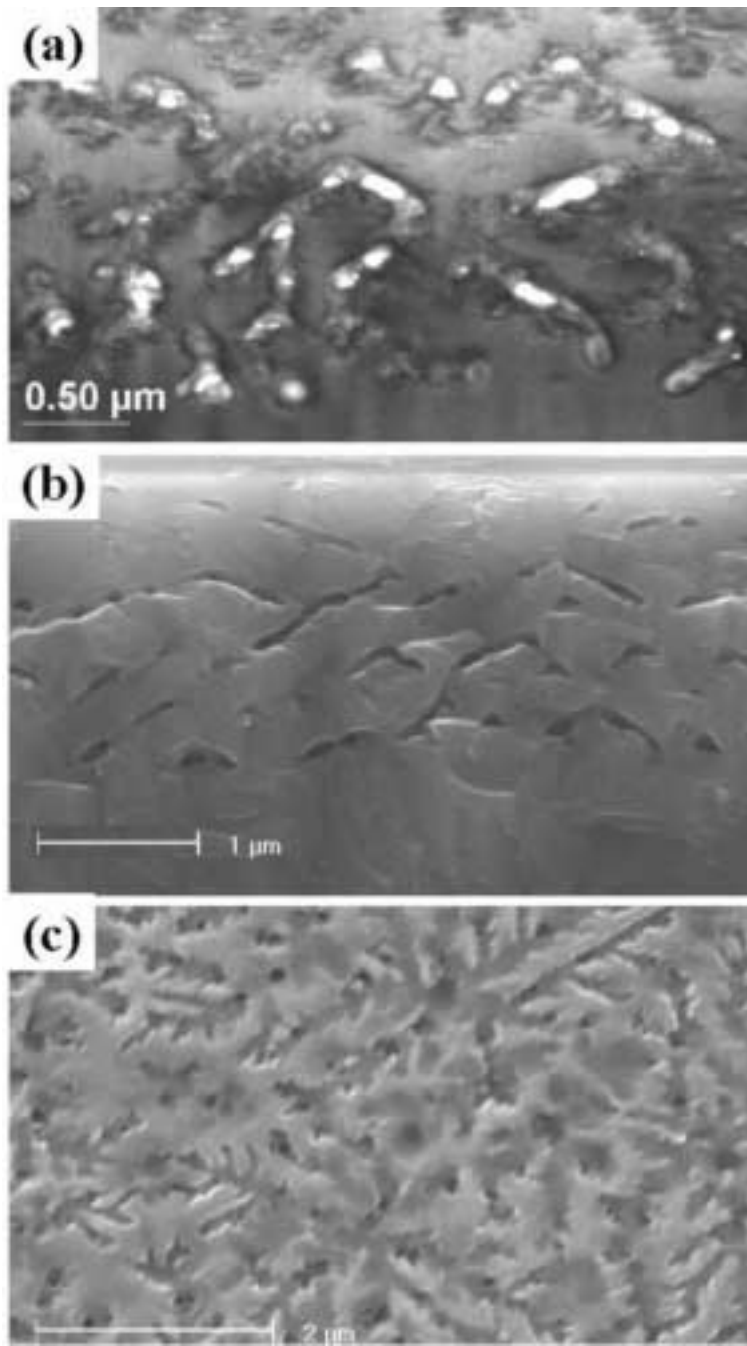


Figure 4. Images of an sparse porous layer in 6H-SiC. (a) Cross-sectional TEM image. (b) Cross-sectional SEM image. The scale marker shows a length of 1 μm . (c) Plan-view SEM image after reactive ion etching. The scale marker shows a length of 2 μm . The sample resistivity is 0.148 $\Omega\text{-cm}$.

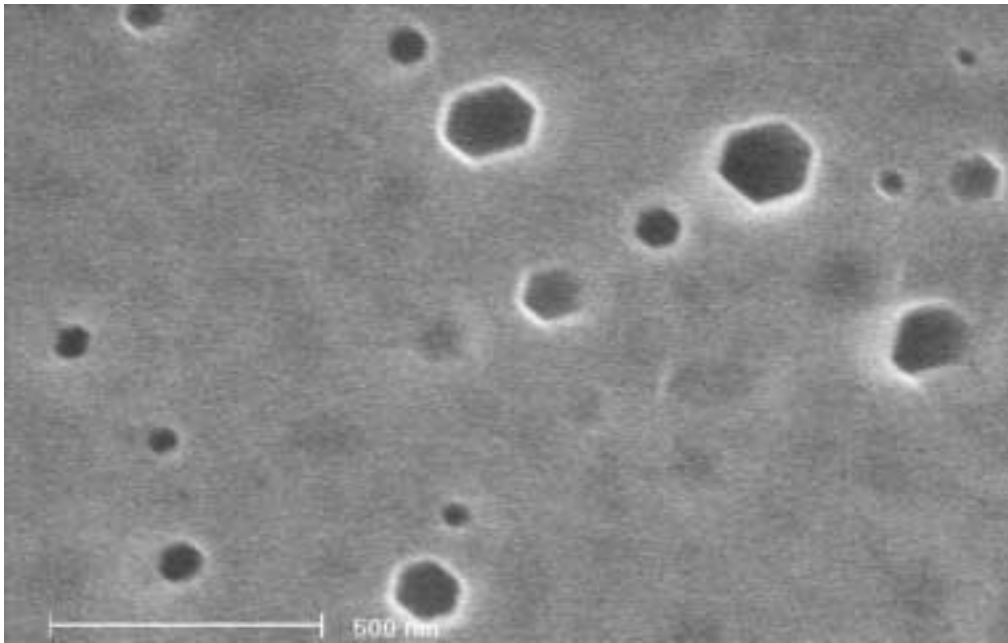


Figure 5. Plan-view SEM image of H-etched surface of porous 4H-SiC. Pores have opened up after 60 seconds of etch at 1680°C. The average pore size is about 100 nm and the surface porosity is about 3.5%. A cross-sectional view of the same sample is shown in Fig. 6(a). The scale marker shows a length of 500 nm.

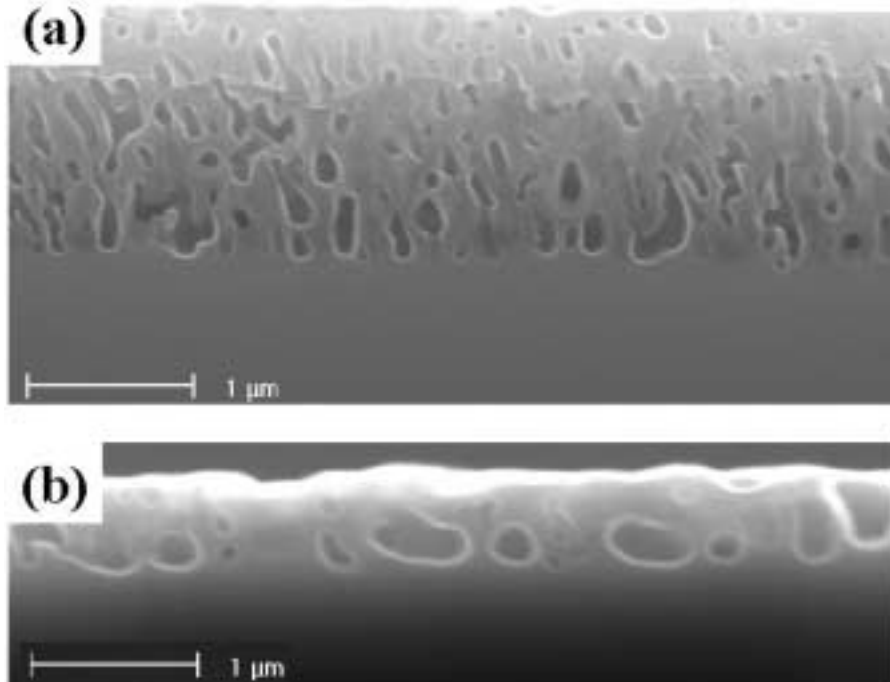


Figure 6. Cross-sectional SEM images of porous 4H-SiC H-etched at 1680°C for (a) 60 s and (b) 300 s. The bulk porosity is about (a) 18% and (b) 31%. The pores have enlarged after etching.

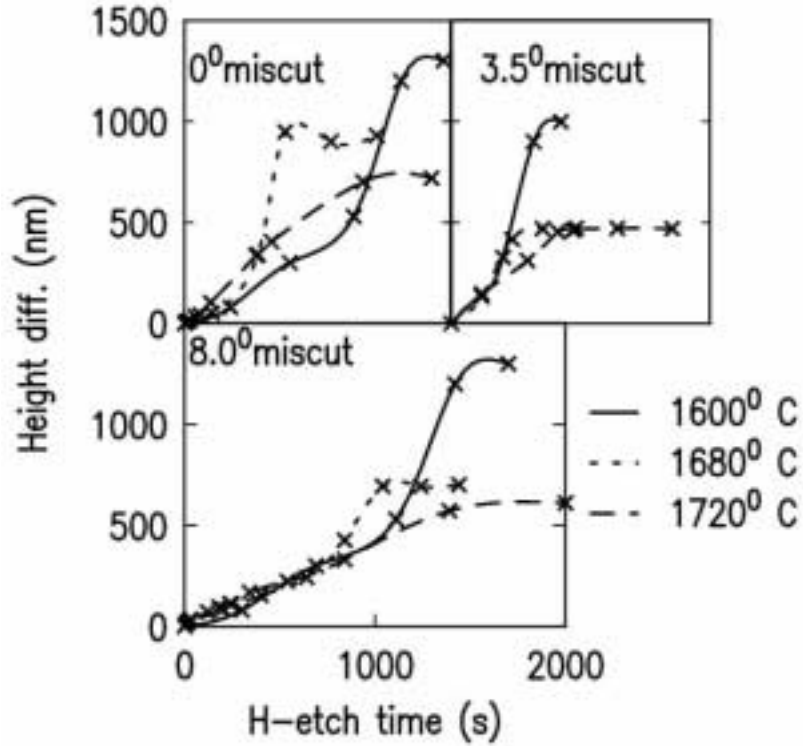


Figure 7. Height difference between porous and nonporous SiC during H-etching for samples with different miscuts and at three different temperatures. Different symbols are used for each temperature, as shown. Lines connecting symbols are drawn as guides to the eye. Samples with 0° and 3.5° miscut are 6H-SiC, and the sample with 8° miscut is 4H-SiC. The time axis is the same for all three plots.